Rb family proteins enforce the homeostasis of quiescent hematopoietic stem cells by repressing Socs3 expression

Eunsun Kim,[1,4] Ying Cheng,[1,5] Elisabeth Bolton-Gillespie,[1] Xiongwei Cai,[6] Connie Ma,[1] Amy Tarangelo,[1] Linh Le,[1,4] Madhumita Jambhekar,[1] Pichai Raman,[2] Katharina E. Hayer,[2] Gerald Wertheim,[3] Nancy A. Speck,[6,7] Wei Tong,[1,5] and Patrick Viatour[1,4]

[1]Center for Childhood Cancer Research, [2]Department of Biomedical and Health Informatics, and [3]Department of Pathology, Children's Hospital of Philadelphia, Philadelphia, PA
[4]Department of Pathology and Laboratory Medicine, [5]Department of Pediatrics, [6]Department of Cell and Developmental Biology, and [7]Abramson Family Cancer Research Institute, Perelman School of Medicine, University of Pennsylvania, Philadelphia, PA

Prolonged exit from quiescence by hematopoietic stem cells (HSCs) progressively impairs their homeostasis in the bone marrow through an unidentified mechanism. We show that Rb proteins, which are major enforcers of quiescence, maintain HSC homeostasis by positively regulating thrombopoietin (Tpo)–mediated Jak2 signaling. Rb family protein inactivation triggers the progressive E2f-mediated transactivation of *Socs3*, a potent inhibitor of Jak2 signaling, in cycling HSCs. Aberrant activation of *Socs3* impairs Tpo signaling and leads to impaired HSC homeostasis. Therefore, Rb proteins act as a central hub of quiescence and homeostasis by coordinating the regulation of both cell cycle and Jak2 signaling in HSCs.

The Journal of Experimental Medicine

INTRODUCTION

Hematopoietic stem cells (HSCs) are highly quiescent and can occasionally enter the cell cycle to either self-renew or differentiate into intermediary progenitor cells (Morrison and Scadden, 2014). In vivo studies have shown that progression through a unique round of cell cycle is not detrimental for HSC homeostasis (i.e., the size of the HSC pool). In contrast, prolonged exit from quiescence progressively impairs the self-renewal and engraftment capacity of proliferative HSCs, which ultimately disrupts their homeostasis in the BM. These observations have fueled the hypothesis that a common yet undefined mechanism enforces both the cellular quiescence and homeostasis of HSCs in the BM (Orford and Scadden, 2008).

The HSC niche provides growth factors and cytokines to modulate HSC fate. In particular, HSCs rely on the binding of the thrombopoietin (Tpo; Tong et al., 2007) cytokine to its receptor Mpl to promote their self-renewal and homeostasis in the BM. Mpl is devoid of any kinase activity and thus recruits the Jak2 kinase to activate several intracellular cascades (Mapk, Akt, and Stat pathways) upon Tpo binding (Vila-Coro et al., 1999; Bersenev et al., 2008). Accordingly, genetic inactivation of *Mpl* (Kimura et al., 1998), *Jak2* (Akada et al., 2014), and *Stat5* (Wang et al., 2009) leads to impaired HSC homeostasis and progressive BM failure. In addition to these positive cues, Jak2 is also negatively regulated by suppressor of cytokine signaling (Socs) proteins (Kershaw et al., 2013) and Lnk. Inactivation of *Lnk* increases Jak2 activity and the size of the HSC pool in the BM (Bersenev et al., 2008). Therefore, it appears that Jak2 plays a central role in the regulation of HSC pool size and that a balance of positive and negative regulators of Jak2 activity controls HSC homeostasis in the BM.

Rb proteins (Rb, p107, and p130) enforce the cellular quiescence of HSCs by repressing the activity of E2f transcription factors through physical interaction (Burkhart and Sage, 2008; Chen et al., 2009). Mitogen stimulation of quiescent HSCs leads to dissociation of the Rb/E2f complex, followed by E2f-mediated activation of a transcriptional program that drives the progression of HSCs through the G_1/S restriction point, by which the fate (self-renewal vs. differentiation) of the daughter cells is thought to be determined (Pietras et al., 2011). However, whether and how E2f factors also govern cell fate determination during progression through the cell cycle is unknown (Chen et al., 2009). In addition, proliferative HSCs are mobilized into the peripheral circulation, suggesting that their retention in the niche may be altered upon entry into the cell cycle (Passegué et al., 2005).

Taking advantage of conditional *Rb* family–deficient mice (triple KO [TKO]), we previously demonstrated that Rb protein inactivation in adult HSCs leads to their robust proliferation and impaired engraftment (Viatour et al., 2008). Using these TKO mice, we now show that Rb proteins collectively maintain HSC homeostasis by promoting the activity of Jak2 downstream of Tpo signaling through repression of E2f-mediated activation of *Socs3* expression. Accordingly, inactivation of the Rb family in HSCs progressively impairs their homeostasis, which is rescued upon repression of *Socs3*

Correspondence to Patrick Viatour: viatourp@email.chop.edu

Abbreviations used: 5-FU, 5-fluorouracil; ChIP, chromatin immunoprecipitation; CT, control; HSC, hematopoietic stem cell; TKO, triple KO; Tpo, thrombopoietin.

The Rockefeller University Press $30.00
J. Exp. Med. 2017 Vol. 214 No. 7 1901–1912
https://doi.org/10.1084/jem.20160719

expression in TKO HSCs. Collectively, our results elucidate a long-awaited mechanism by showing that Rb proteins enforce the homeostasis of quiescent HSCs in the BM by repressing distinct transcriptional programs regulated by E2f factors.

RESULTS AND DISCUSSION

Rb proteins maintain quiescence and homeostasis in HSCs

We inactivated the entire Rb family of genes in all hematopoietic cells by deleting *Rb* and *p130* alleles in $Rb^{Lox/Lox}$ $p130^{Lox/Lox}$ $p107^{-/-}$ mice using a tamoxifen-regulated Cre recombinase expressed from the Rosa26 locus (Rosa26-CreER^{T2}). Here, we refer to hematopoietic cells with Rb family deletion as TKO cells. We observed unaltered frequency of phenotypic TKO progenitors (lineage$^-$ Kit$^+$ Sca1$^+$ Cd48$^+$ Cd150$^-$) and HSCs (lineage$^-$ Kit$^+$ Sca1$^+$ Cd48$^-$ Cd150$^+$) relative to control (CT; provided by tamoxifen-treated $Rb^{Lox/Lox}$ $p130^{Lox/Lox}$ $p107^{-/-}$ mice, which are phenotypically and functionally indistinguishable from WT mice; Fig. S1) populations 2 wk after deletion (Fig. 1 A) despite their increased proliferative activity (Fig. 1, B and C). To assess the growth potential of TKO HSCs in vitro, we plated unfractioned BM and purified HSCs isolated from CT and TKO mice 2 wk after tamoxifen treatment in semisolid culture for colony assay. TKO cells initially exhibited increased colony-forming activity, but serial replating of a fixed number of cells resulted in faster exhaustion of their colony-forming activity compared with CT (Fig. 1 D and Fig. S2 A). To rule out nonhematopoietic priming of TKO HSCs before collection from BM, we isolated unfractioned BM cells from untreated CT and TKO mice and determined their colony-forming activity in the presence of 4-OH-tamoxifen. Upon successful recombination of floxed alleles (not depicted), TKO cells displayed impaired colony-forming activity compared with CT (Fig. S2 B). Altogether, these data suggest that, after an initial phase of expansion, TKO HSCs and their downstream progenitors exhaust prematurely in vitro.

Expression of the Rosa26 locus is ubiquitous (Casola, 2010), leading to a widespread Rb family inactivation and the subsequent early mortality of Rosa26Cre-ER^{T2} TKO mice. To circumvent this early mortality (which prevents long-term in vivo study) and avoid potential non–cell-autonomous phenotypes, we transplanted unrecombined BM cells from CT and TKO mice into lethally irradiated immunocompromised hosts. ($Rag1^{-/-}$ mice were used as recipients to overcome the transplantation issues associated with the mixed 129/BL6 background of TKO mice; these mice are defined as CT and TKO chimeras based on the origin of the transplanted BM cells.) Upon establishment of hematopoiesis (5 wk), recipient mice were treated with tamoxifen and killed at predetermined time points to analyze hematopoiesis and the HSC compartment (Fig. 1 E). Whereas the BM pool of progenitors in both groups was stable during the course of the experiment, TKO HSC frequency initially remained stable during the first 2 wk, then progressively decreased to approximately a tenth of the CT HSC frequency by the 8-wk time point (Fig. 1, F and G; and Fig. S2 C). HSCs isolated from TKO chimeras at 8 wk displayed decreased colony-forming activity compared with CT, whereas the colony-forming activity of progenitors was unaffected (Fig. 1 H and Fig. S2 D). However, TKO cells did not display increased apoptosis compared with CT (Fig. S2 E). These data indicate that, in addition to decreased frequency, TKO HSC are also functionally impaired in their capacity to form colonies.

Recent data have highlighted the predominant role of HSCs for hematopoiesis upon transplantation (Sun et al., 2014; Busch et al., 2015). However, histological analysis reveals a modest decrease in the BM cellularity of TKO chimeras compared with CT (Fig. S2, F and G), with a reduced percentage of lymphoid cells in TKO chimeras compared with CT (Fig. 1 I). In the spleen, expansion of the red pulp, which is suggestive of extramedullary hematopoiesis (O'Malley et al., 2005), was observed in TKO chimeras at 4 wk but not 18 wk (Fig. 1 J). At the 18-wk time point, TKO chimera spleens were enlarged and contained a higher number of HSCs and progenitor compared with CT (Fig. 1, K and L), which is associated with higher colony-forming activity of TKO splenocytes compared with CT (Fig. 1 M). Yet, the colony-forming activity from TKO chimera spleen was marginal compared with the activity observed from CT and TKO chimera BM (Fig. 1 N). When cellularity from both BM and spleen is combined, 10–20% of TKO HSCs were still present in the BM, and another 20–25% were present in the spleen, compared with CT (Fig. 1 O). Collectively, these data indicate that upon Rb family inactivation, a significant fraction of HSCs exit the BM to occupy the spleen. However, after a brief period of hematopoiesis, their contribution to blood cell formation appears to be limited.

Finally, we generated additional chimeras and, 5 wk after tamoxifen treatment, performed weekly injection with the myeloablative agent 5-fluorouracil (5-FU; Fig. 1 P). In these conditions, TKO chimeras displayed early mortality compared with CT (Fig. 1 Q), indicating that inactivation of Rb family proteins impairs the resistance of HSC to stress-induced hematopoiesis.

Socs3 is an E2f target gene activated upon sustained E2f activity in HSCs

To elucidate the molecular mechanism by which Rb proteins maintain the homeostasis of quiescent HSCs, we performed array analyses on flow-purified HSCs from CT and TKO mice 2 wk after tamoxifen treatment (Table S1). GSEA analysis of the genome-wide array data (see Tables S2 and S3 for full results) identified cell cycle and E2f target genes as the most enriched gene sets in TKO HSCs compared with CT. The third most highly enriched gene set corresponded to regulators of cytokine signaling (Fig. 2 A) and, from this gene set, *Socs3* was the most highly up-regulated mRNA in TKO HSCs compared with CT (Fig. 2 B; and Table S1). RT-qPCR analysis confirmed increased expression of *Socs3* in TKO HSCs compared with CT and showed that *Socs3* transac-

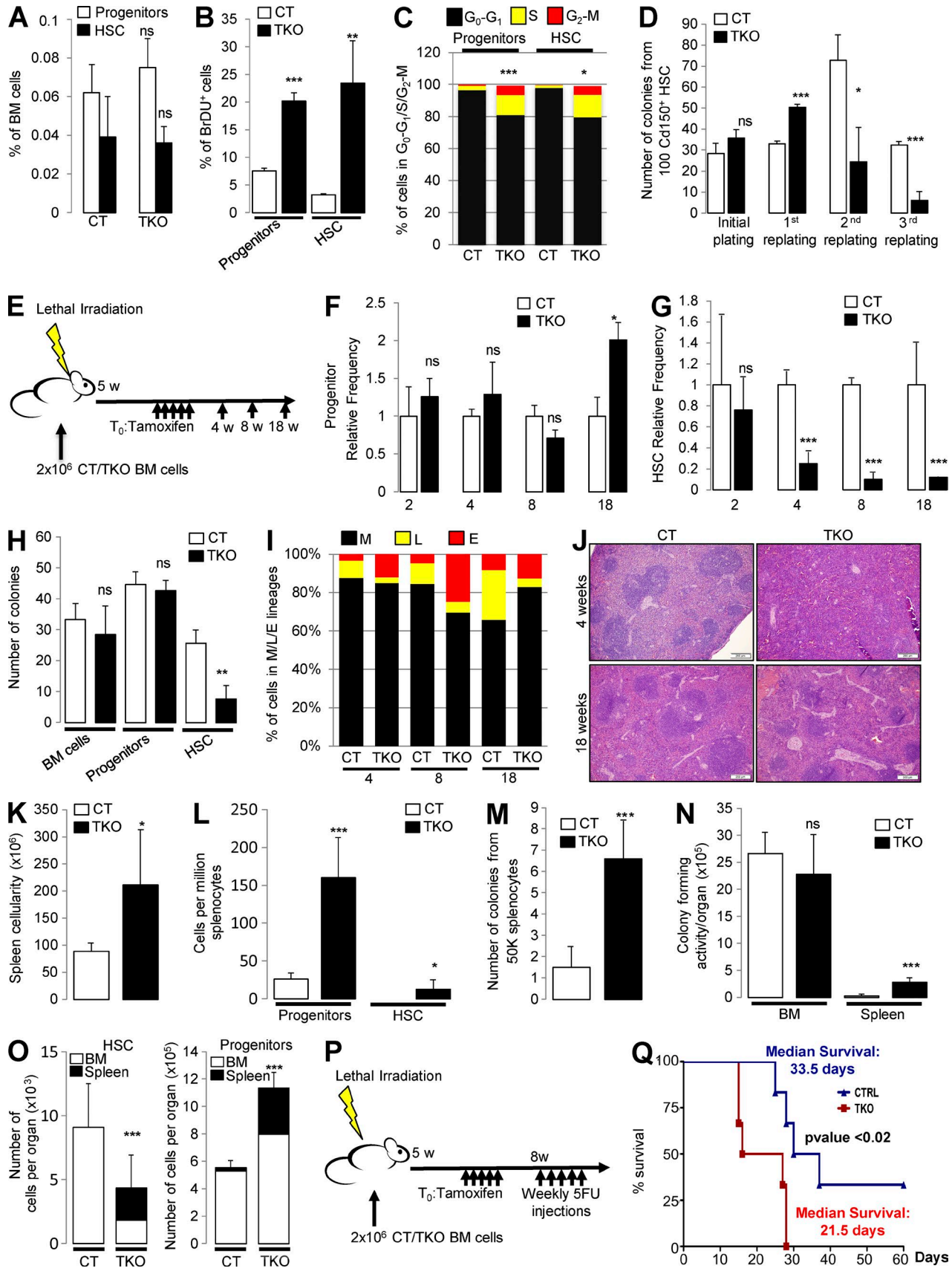
A
Progenitors
HSC
% of BM cells
CT
TKO
ns
B
CT
TKO
% of BrDU+ cells
Progenitors
HSC
C
G0-G1
S
G2-M
Progenitors
HSC
% of cells in G0-G1/S/G2-M
D
CT
TKO
Number of colonies from 100 Cd150+ HSC
Initial plating
1st replating
2nd replating
3rd replating
E
Lethal Irradiation
5 w
T0:Tamoxifen
4 w 8 w 18 w
2x10^6 CT/TKO BM cells
F
CT
TKO
Progenitor Relative Frequency
G
CT
TKO
HSC Relative Frequency
H
CT
TKO
Number of colonies
BM cells
Progenitors
HSC
I
M
L
E
% of cells in M/L/E lineages
J
CT
TKO
4 weeks
18 weeks
K
CT
TKO
Spleen cellularity (x10^6)
L
CT
TKO
Cells per million splenocytes
Progenitors
HSC
M
CT
TKO
Number of colonies from 50K splenocytes
N
CT
TKO
Colony forming activity/organ (x10^5)
BM
Spleen
O
HSC
BM
Spleen
Number of cells per organ (x10^3)
Progenitors
BM
Spleen
Number of cells per organ (x10^5)
P
Lethal Irradiation
5 w
8w
T0:Tamoxifen
Weekly 5FU injections
2x10^6 CT/TKO BM cells
Q
Median Survival: 33.5 days
CTRL
TKO
pvalue <0.02
Median Survival: 21.5 days
% survival
Days

tivation is predominantly restricted to TKO HSC, as *Socs3* expression barely increases in TKO progenitors (Fig. 2 C). Because *Socs3* overexpression enforces the differentiation of embryonic stem cells by inhibiting Jak2 activity downstream of Lif signaling (Li et al., 2005), we reasoned that *Socs3* may represent a valid candidate for the regulation of proliferative HSC homeostasis. To understand the molecular mechanism of *Socs3* up-regulation in TKO HSCs, we screened the *Socs3* promoter region and identified an E2f binding site in the proximity of the transcription start site that is conserved among several *Socs* gene promoters (Fig. 2 D). Analysis of previously published chromatin immunoprecipitation (ChIP)–Seq data identified the binding of E2f1 to the *Socs3* promoter in breast cancer (Cao et al., 2011) and liver cancer (Tarangelo et al., 2015) cell lines, but analysis of expression data showed a lack of *Socs3* transactivation in Rb family–deficient hepatocellular carcinoma (TKO HCC; Tarangelo et al., 2015), suggesting a cell type–specific transactivation of *Socs3* by E2f. In addition, ChIP experiments in unfractioned primary BM cells and myeloid progenitor–derived 32D cells, as well as luciferase assays in 293 cells, confirmed that E2f factors bind to and transactivate the *Socs3* promoter (Fig. 2, E–G), thereby establishing *Socs3* as a novel E2f target gene.

We recently identified two classes of E2f target genes defined as early and late targets (Tarangelo et al., 2015). Although late E2f target genes (primarily activated upon prolonged E2f activity and enriched for non–cell cycle functions) harbor only a minimal E2f core binding site (-CGCGC-), early E2f target genes (promptly activated upon transient E2f activity and predominantly enriched for cell cycle functions) harbor a thymidine (T)-stretch at the 5′ extremity of a minimal E2f core binding site that confers high E2f affinity binding (Tarangelo et al., 2015). The E2f binding site located in the *Socs3* promoter includes a degenerated T-stretch, suggesting that *Socs3* is a late E2f target gene; accordingly, inserting a T-stretch in the E2f binding site improved the binding affinity of recombinant E2f1 (Fig. 2 H). In addition, minimum competition (1:2 ratio) by a cold E2f consensus probe was sufficient to disrupt the E2f–*Socs3* probe complex (Fig. 2 I). In agreement with the delayed activation kinetics of late E2f target genes, *Socs3* expression was not activated in proliferative TKO HSCs 4 d after Rb family inactivation (Fig. 2 J). Accordingly, expression analysis of HSCs isolated at different time points after their stimulation with 5-FU showed the rapid induction of a cell cycle signature peaking at day 6 (in agreement with the findings of the authors) in the absence of any significant *Socs3* transactivation (Fig. 2 K; Venezia et al., 2004). Collectively, these data identify *Socs3* as a novel E2f target gene in HSCs that is activated only in the context of sustained E2f activity.

Rb proteins maintain the intracellular response to Tpo and Sdf1 signaling

To test the consequences of increased *Socs3* expression on TKO HSC homeostasis, we determined the activity of cytokines Tpo and Sdf1 (which is critical for HSC engraftment and retention in the BM; Sugiyama et al., 2006) that recruit Jak2 in HSCs and other cell types (Fig. 3 A; Vila-Coro et al., 1999; Pello et al., 2006; Bersenev et al., 2008), in CT and TKO cells isolated 2 wk after tamoxifen treatment. Stimulation with Tpo led to reduced Jak2 phosphorylation in TKO KLS (lineage$^-$ Kit$^+$ Sca1$^+$) cells, compared with CT (Fig. 3 B). Using p-Stat5 and p-S6 as readouts for Jak2 activity in progenitors and HSCs, we found that stimulation

Figure 1. **Impaired homeostasis of TKO HSCs.** (A) BM cells were isolated from CT (left) and TKO (right) mice 2 wk after tamoxifen injection. Frequency of progenitor cells and HSCs was determined by flow cytometry (Student's *t* test; *n* = 3 mice per group). (B and C) 2 wk after tamoxifen injection, CT and TKO mice were injected with BrdU 4 h before euthanasia. Flow-isolated progenitors and HSCs were incubated with BrdU (B) and propidium iodide (PI; C) for cell cycle analysis (Student's *t* test; *n* = 3 mice per group). (D) 100 flow-isolated HSCs were obtained from CT and TKO mice 2 wk after tamoxifen injection and plated in methylcellulose. Colonies were counted after 9 d, and 10,000 cells were replated for serial replating analysis (Student's *t* test; *n* = 3). (E) BM cells from CT and TKO mice were transplanted into conditioned *Rag1*$^{-/-}$ mice. 5 wk after transplant, chimeras were injected with tamoxifen, and BM cells from chimeras were collected at different time points after tamoxifen injection for analysis. (F and G) Relative frequency of progenitors (F) and HSCs (G) in CT and TKO chimeras at 2, 4, 8, and 18 wk after tamoxifen treatment (Student's *t* test; *n* = 4 mice per genotype per time point). (H) 10,000 BM cells, 100 progenitors, and 100 HSCs from CT and TKO chimeras were isolated 8 wk after tamoxifen treatment and plated in methylcellulose. Colony formation was determined 9 d after plating (Student's *t* test; *n* = 3). (I) Frequency of myeloid (M), lymphoid (L), and erythroid (E) cells in the BM of chimeras at different time points after tamoxifen treatment, as identified by a combination of surface markers and size analysis (Student's *t* test; *n* = 4 mice per genotype per time point). (J) Histology of spleen from CT (left) and TKO (right) chimeras 4 wk (top) and 18 wk (bottom) after tamoxifen treatment, as identified by hematoxylin and eosin staining (three spleens per genotype per time point were assessed). Bars, 200 µm. (K) Spleen cellularity in CT and TKO chimeras 18 wk after tamoxifen treatment (Student's *t* test; *n* = 5 mice per genotype). (L) Number of progenitors and HSCs per million splenocytes, as identified by a combination of flow cytometry and total spleen cellularity 18 wk after tamoxifen treatment (Student's *t* test; *n* = 5 mice per genotype). (M) 50,000 splenocytes from CT and TKO chimeras isolated 18 wk after tamoxifen treatment were plated in methylcellulose, and colonies were counted after 9 d in culture (Student's *t* test; *n* = 3). (N) Colony-forming activity/organ was obtained by integrating colony-forming activity per 10,000 (BM) and 50,000 (spleen) cells with the total cellularity per organ (Student's *t* test; *n* = 3). (O) Total numbers of HSCs and progenitors per organ were obtained by integrating the frequency of HSC and progenitors (per million, as quantified by flow cytometry) with the total cellularity of the corresponding organ 18 wk after tamoxifen treatment. The combined number of HSCs and progenitors identified in BM and spleen is displayed (Student's *t* test; *n* = 5 mice per genotype). (P) Experimental protocol to study the resistance of CT and TKO chimeras under 5-FU–induced stress conditions. Conditioned *Rag1*$^{-/-}$ mice were transplanted with BM cells from CT and TKO mice. 5 wk after transplant, chimeras were treated with tamoxifen. 8 wk after tamoxifen treatment, recipient mice were injected weekly with 5-FU. (Q) Survival curve (log-rank test; *n* = 5 mice per genotype). Error bars represent standard deviation. *, P < 0.05; **, P < 0.01; ***, P < 0.001.

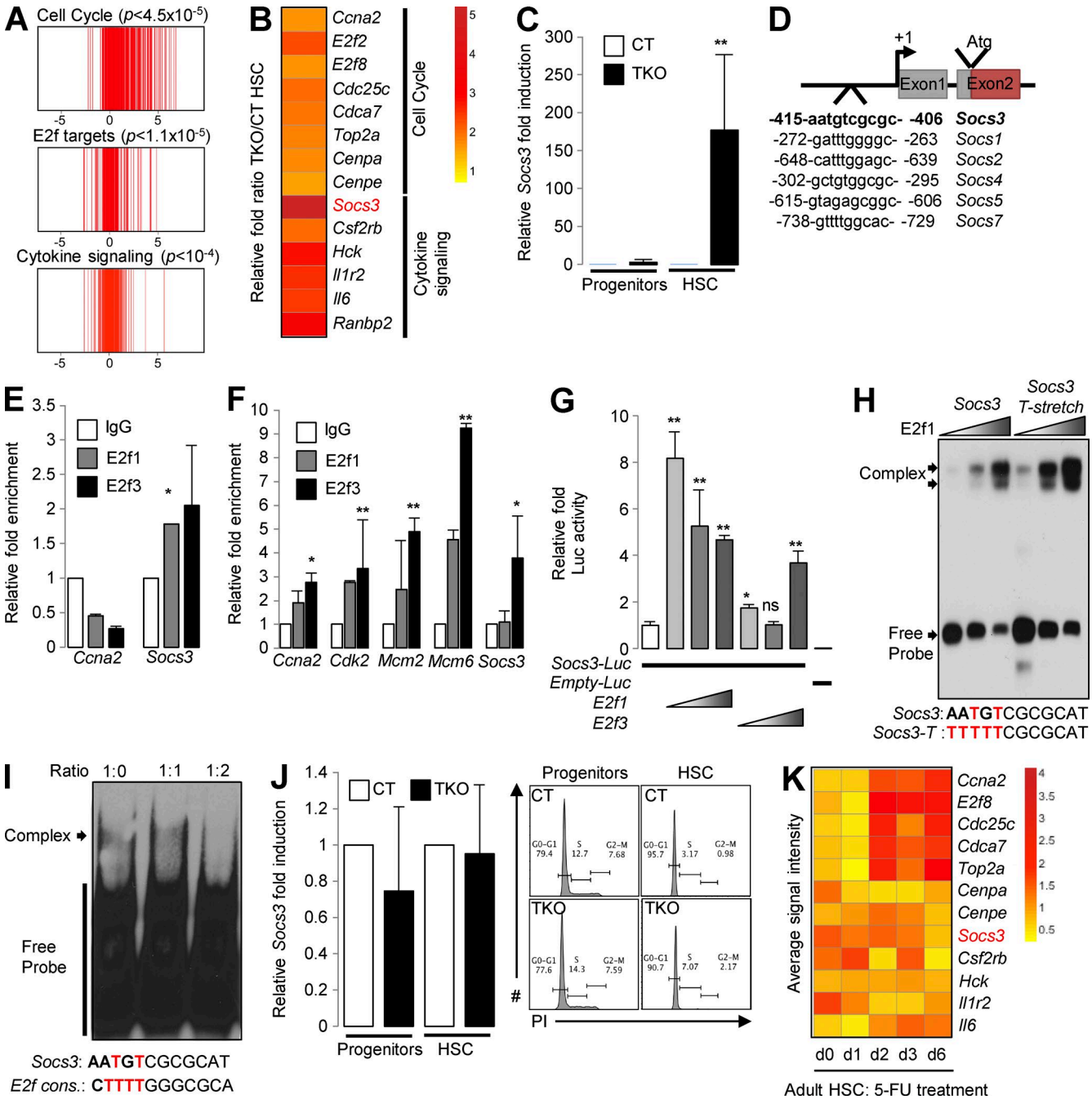

Figure 2. ***Socs3* is an E2f target gene.** (A) GSEA profiles of the most significant gene sets enriched in flow-isolated TKO HSCs compared with CT 2 wk after tamoxifen treatment of CT and TKO mice. Each vertical bar represents a gene from the gene set, and its fold activation in TKO versus CT HSCs is indicated by its position on the vertical axis. The full list of gene set enrichment is displayed in Table S1. (B) Heat map for representative cell cycle genes and the cytokine signaling gene set activated in TKO HSCs compared with CT. Fold induction is displayed in the log2 base. (C) *Socs3* expression in CT and TKO HSCs and progenitors 2 wk after tamoxifen treatment, as detected by qPCR (Student's *t* test; $n = 3$ samples per genotype). (D) Representation of *Socs3* regulatory region. A putative E2f-binding site is identified in the position −415 to −406 upstream of the transcription start site. Similar E2f-binding sites are located in the regulatory region of other *Socs* genes. (E) ChIP assay performed in primary BM white blood cells to pull down endogenous E2f1 and E2f3 at the promoter of *Ccna2* and *Socs3* (Student's *t* test; $n = 2$). (F) ChIP assay performed in 32D progenitor cells to pull down endogenous E2f1 and E2f3 at the promoter of *Ccna2*, *Cdk2*, *Mcm2*, and *Mcm6* (all validated E2f target genes; Tarangelo et al., 2015) and *Socs3* (Student's *t* test; $n = 3$). (G) Transactivation of a 1.6-kb mouse *Socs3* promoter cloned upstream of the luciferase cDNA by increasing amount of transfected E2f1 and E2f3, as shown by luciferase assay. Empty pGl3-Luc vector was used as a negative CT (Student's *t* test; $n = 4$). (H) Gel shift assay with stable amount of probes containing either the original E2f-binding site found in the *Socs3* promoter (*Socs3*) or a mutated version of this binding site where a T-stretch has been added to the minimal

with Tpo led to decreased phosphorylation of Stat5 and S6 in TKO cells compared with CT (Fig. 3, C and D). These results therefore show that Tpo/Mpl/Jak2 signaling is impaired in TKO HSCs and progenitors. In addition, TKO KLS cells exhibited impaired migration capacity when placed in a Sdf1 gradient (Fig. 3 E), indicating defective Sdf1 signaling in these cells. However, intracellular signaling analysis revealed a lack of Jak2 and Fak (Glodek et al., 2007; another Socs3 target [Le et al., 2007]) activation upon Sdf1 stimulation in KLS cells, suggesting that Sdf1 may activate an alternative signaling pathway in hematopoietic progenitors (Fig. 3 F).

In contrast to TKO HSCs, TKO progenitors only exhibited reduced Jak2 activity upon exposure to a high Tpo dose (20 ng/ml; Fig. 3, C and D), which correlates with the limited transactivation of *Socs3* in TKO progenitors (see Fig. 2 C) and KLS cells (which contain a majority of progenitors; Fig. 3 G). Remarkably, global comparison of gene signatures in TKO HSCs and KLS cells versus their respective CTs indicated that the transcriptional output is extremely different between TKO HSCs and progenitor cells, with only 21 genes up-regulated in both HSC and KLS cells upon Rb family inactivation. In contrast, 336 and 364 genes are uniquely up-regulated in TKO HSC and TKO KLS cells, respectively (Fig. 3 H; see Tables S4, S5, and S6 for full gene lists). These differentiation stage–specific gene signatures each combine distinct cell cycle genes (Table S7) as well as genes associated with non–cell cycle functions, such as *Socs3*. These data suggest that the transcriptional consequences of Rb family inactivation, predominantly driven by E2f, include both the activation of a common cell cycle program (although driven by different cell cycle genes) and the cell type–specific activation of non–cell cycle features.

Finally, fetal liver HSCs retain self-renewal potential despite their sustained proliferation, suggesting that the mechanisms linking quiescence and homeostasis may be different in fetal versus adult HSCs. Accordingly, whereas fetal liver HSCs activated a robust cell cycle signature compared with their adult counterparts, they failed to transactivate *Socs3* expression (Fig. 3 I; Venezia et al., 2004). Collectively, these results suggest that *Socs3* transactivation by E2f factors is restricted to adult HSCs.

Level of *Socs3* expression dictates HSC homeostasis in the BM

To functionally test the consequences of increased *Socs3* expression on the regulation of TKO HSC homeostasis, we genetically manipulated *Socs3* expression in CT and TKO KLS cells in vitro and in vivo. We found that *Socs3* overexpression decreased the number and size of colonies formed by transduced CT and TKO cells in methylcellulose culture (Fig. 4, A and B) and increased the frequency of lineage-specific colonies (granulocyte, macrophage, granulocyte-macrophage, colony-forming unit erythrocyte, burst-forming unit, and megakaryocyte) at the expense of mixed-lineage colonies (granulocyte-erythrocyte-monocyte-megakaryocyte; Fig. 4 B). Similarly, overexpression of *Socs3* in CT lineage$^-$ Kit$^+$ (KL) cells followed by their transplantation into recipient mice decreased the frequency of HSCs but not their downstream progenitors, as shown by the unaltered frequency of KLS cells (Fig. 4 C). Together, these data indicate that overexpression of *Socs3* impairs HSC homeostasis in the BM.

We then performed the opposite experiment via shRNA-mediated silencing of *Socs3* expression (using two different hairpins to silence *Socs3* in parallel with a *Scramble* hairpin; Cui et al., 2011) in CT and TKO KLS cells. Partial repression (~65% knockdown) of *Socs3* expression had no significant effect on the colony-forming capacity of transduced CT and TKO cells in vitro, except for a mild twofold reduction in the number of colonies generated by transduced TKO cells upon expression of the *Socs3* hairpin #2 (Fig. 4 D). However, *Socs3* repression increased the frequency of mixed-lineage colonies from both transduced CT and TKO cells at the expense of lineage-specific colonies (Fig. 4 E). Silencing of *Socs3* in TKO KL cells followed by their transplantation into recipient mice led to an approximately 10-fold expansion of both TKO progenitors and TKO HSCs compared with the corresponding TKO populations infected with the *Scramble* vector 9 wk after tamoxifen injection of recipient mice (Fig. 4 F; compare with ~10-fold reduction of HSC frequency at 8 wk in Fig. 1 G). However, long-term (30 wk) follow-up did not show any aberrant accumulation of *Socs3* shRNA-transduced TKO cells in the BM of recipient mice compared with Scramble shRNA-transduced TKO cells (Fig. 4 G). This latest result suggests that the silencing of *Socs3* in proliferative TKO HSCs is sufficient to restore their homeostasis in the BM without inducing cellular transformation.

Concluding remarks

Through its regulation of Tpo signaling, Jak2 plays a critical role in preserving HSC homeostasis in the BM (Pello et al.,

-CGCGC- core binding site (*Socs3 T-stretch*), together with increasing amount of recombinant GST-E2f1. The sequences of both binding sites are under the autoradiogram. The free probe and the E2f1–probe complexes are indicated by their respective arrows. (I) Competition gel shift assay between a fixed amount of the biotin-labeled *Socs3* probe and an increasing amount of an unlabeled probe containing a consensus E2f-binding site (first lane, absent; second lane, amount equal to the biotin-labeled probe; third lane, twofold amount of the biotin-labeled probe), together with 5 µg of nuclear extracts isolated from primary BM white blood cells. (J) *Socs3* expression (left) and cell cycle activity (right) in CT and TKO HSCs/progenitors 4 d after tamoxifen treatment, as detected by qPCR (Student's *t* test; $n = 2$ samples per genotype) and propidium iodide (PI) incorporation assay ($n = 3$ mice per genotype). *Gapdh* expression serves as normalization gene. (K) Heat map for a representative set of cell cycle genes and the cytokine signaling gene set in adult HSCs at different time points after 5-FU treatment. Fold induction is displayed in the log2 base. Error bars represent standard deviation. *, $P < 0.05$; **, $P < 0.01$.

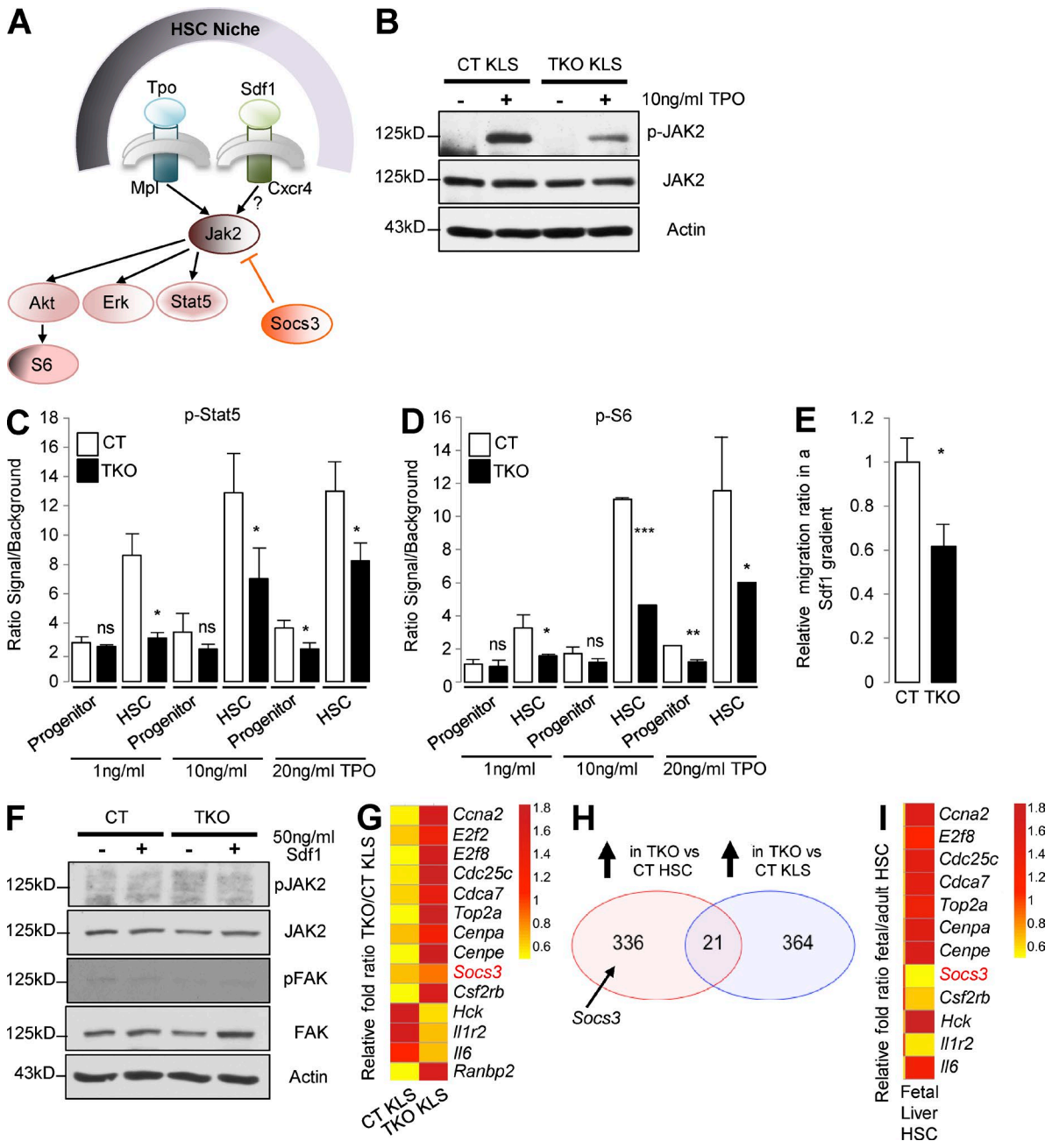

Figure 3. **Impaired cytokine activity in TKO HSCs.** (A) Diagram of Tpo and Sdf1 signaling pathways in HSCs. (B) KLS cells were isolated from CT and TKO mice 2 wk after tamoxifen treatment, placed in liquid culture, serum-starved for 1 h, and treated with 10 ng/ml Tpo for 10 min. p-Jak2, total Jak2, and actin (normalization) were detected in total cell extracts by immunoblotting. (C and D) Progenitors and HSCs were isolated from CT and TKO mice 2 wk after tamoxifen treatment, placed in liquid culture, serum-starved for 1 h, and treated with 1, 10, and 20 ng/ml recombinant Tpo for 10 min. p-Stat5 and p-S6 were assessed by p-flow (Student's *t* test; $n = 3$). (E) KLS cells were isolated from CT and TKO mice 2 wk after treatment with tamoxifen, serum-starved for 1 h, and placed in the upper compartment of a Boyden chamber. KLS cells present in the lower compartment were quantified by flow cytometry after 4 h of migration (Student's *t* test; $n = 3$). (F) KLS cells were isolated from CT and TKO mice 2 wk after treatment with tamoxifen, serum-starved for 1 h, and treated with 50 ng/ml Sdf1 for 2 min. p-Jak2, total Jak2, p-Fak, total Fak, and actin (normalization) were detected in total cell extracts by immunoblotting. (G) Expression analysis of representative cell cycle genes and cytokine signaling genes in CT and TKO KLS cells (Viatour et al., 2008). Fold induction is displayed in the log2 base. (H) Venn diagrams indicating the number of genes up-regulated in TKO HSCs (left) and KLS cells (right) compared with their respective CTs. The full list of genes is available in Table S1. (I) Expression analysis of representative cell cycle genes and cytokine signaling genes in fetal liver HSCs compared with adult HSCs. Fold induction is displayed in the log2 base. Error bars represent standard deviation. *, $P < 0.05$; **, $P < 0.01$; ***, $P < 0.001$.

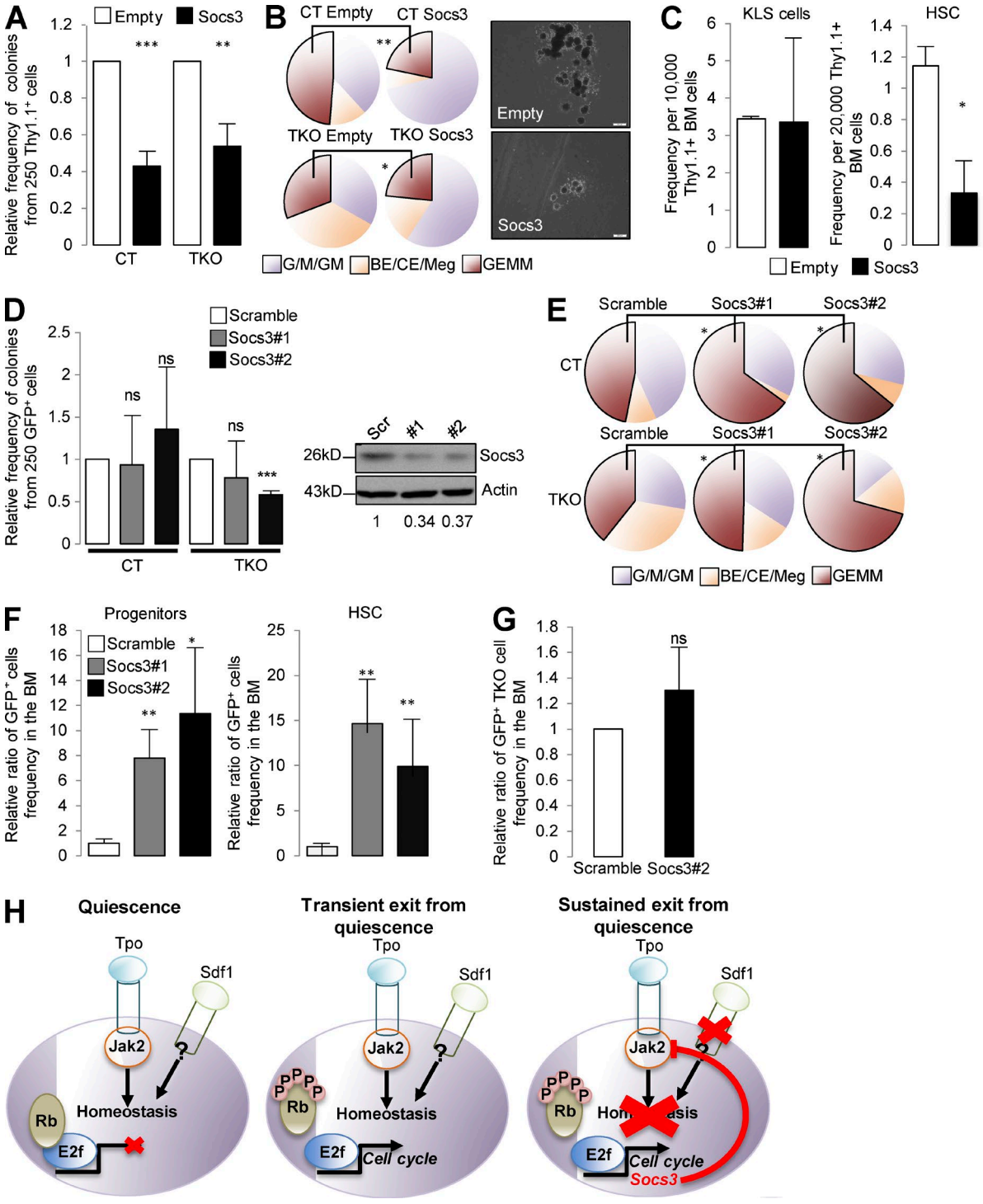

Figure 4. **Modulation of *Socs3* expression impacts the homeostasis of HSCs.** (A) 250 Thy1$^+$ CT and TKO cells transduced with either empty or *Socs3*-expressing vectors were plated in 1 µM methylcellulose$^+$ 4-OH-tamoxifen for colony formation assay. Colony numbers were quantified 9 d after plating (Student's *t* test; $n = 3$). For each genotype, colony-forming activity is displayed as a fold of the colony-forming activity of cells transduced with the empty vector (arbitrarily set at 1). (B, left) Frequency of the different types of colonies formed by CT and TKO cells transduced with either empty or *Socs3*-expressing vectors (Student's *t* test; $n = 3$). (right) Representative colony-forming unit-erythroid (CFU-E) observed in CT cells transduced with either empty (top) or *Socs3*-expressing (bottom) vector. Bars, 200 µm. (C) 4000 Thy1$^+$ CT cells infected with either empty or *Socs3*-expressing vector were transplanted into conditioned recipient mice with BM helper cells. The frequency of Thy1$^+$ KLS cells (left) and Thy1$^+$ HSCs (right) was determined by flow cytometry 9 wk after transplantation (Student's *t* test; $n = 5$ mice per group). (D, left) 250 GFP$^+$ CT and TKO cells infected with a LMP-GFP retroviral vector ex-

2006; de Graaf and Metcalf, 2011; Anthony and Link, 2014). The expression of *Socs3*, a potent inhibitor of Jak2, is low in HSCs, which correlates with the absence of HSC phenotype in *Socs3*-deficient mice (Marine et al., 1999). Proliferative HSCs display impaired homeostasis in the BM, and our data identify a molecular connection establishing Rb proteins as a central hub for the maintenance of quiescence and homeostasis in adult HSCs through the combined repression of cell cycle genes and *Socs3* (Fig. 4 H). In particular, the identification of *Socs3* as a late E2f target gene that requires prolonged E2f activity for its transactivation correlates with the progressive disruption of homeostasis observed by us (Fig. 1 G) and others (Orford and Scadden, 2008) in proliferative HSCs.

Proliferative HSCs are mobilized in the peripheral circulation, and their transplantation potential is compromised (Passegué et al., 2005). Interestingly, our data also show that Sdf1 signaling, which is critical for HSC engraftment in their niche, is impaired in TKO HSCs, although the molecular mechanism remains unclear at this point. Future work will include tailored functional and molecular assays to determine the mechanism and consequence of impaired Sdf1 signaling in TKO HSCs.

Jak2 regulates the activity of multiple cytokines in different blood populations, which suggests that its regulation must be cell type specific to avoid multipopulation consequences (Meyer and Levine, 2014). Our transcriptional data indicate that E2f transcriptional output is highly cell type specific: although activation of a cell cycle program is a common consequence of E2f activity, the variability of E2f transcriptional output through hematopoietic differentiation leads to the HSC-specific activation of *Socs3* and repression of Jak2 activity. Although the molecular basis for this transcriptional variability is not currently known, we hypothesize that it is influenced by the local chromatin conformation. However, more experimental evidence is needed to support this model.

Finally, myeloproliferative neoplasms are predominantly driven by constitutively active Jak2 mutants (Staerk and Constantinescu, 2012; Meyer and Levine, 2014), and the *Socs3* promoter is often methylated during the course of the disease (Capello et al., 2008). Similarly, we hypothesize that activation of *Socs3* expression in proliferative HSCs acts as a tumor suppressor mechanism by enforcing the differentiation of proliferative HSCs to prevent their unnecessary accumulation and potential transformation.

MATERIALS AND METHODS

Mice

Rosa26-CreER^{T2} Rb$^{Lox/Lox}$ p130$^{Lox/Lox}$ p107$^{-/-}$ mice were previously described (Viatour et al., 2008), and Cre expression was induced by intraperitoneal injection of 1 mg tamoxifen (Sigma-Aldrich) in corn oil for five consecutive days. Mice were housed in the Children's Hospital of Philadelphia (CHOP) barrier facility. All experiments were approved by CHOP Institutional Animal Care and Use Committee (protocol 969).

Flow cytometry

Cells from the BM (femur, tibia, and hips) and spleen were filtered, and red blood cells were lysed with ACK buffer ($NH_4Cl/KHCO_3$). The remaining white blood cells were stained with a cocktail of lineage antibodies (CD3, CD4, CD8, B220, Ter119, Mac1, and Gr1) and antibodies against Kit, Sca1, Cd48, and Cd150 (eBioscience). Flow analysis and sorting were performed on an LSR Fortessa and Mowflo, respectively. Cell cycle analysis was performed by injecting mice with BrdU 4 h before death. Cells were processed as previously described (Viatour et al., 2008) and analyzed on an analogue analyzer. Apoptosis assay was performed with the Annexin V Apoptosis Detection kit (eBioscience), according to the manufacturer protocol.

Transplantation and 5-FU assay

Two million unfractioned BM cells were collected from CT and TKO mice and retro-orbitally transplanted into lethally irradiated (8G) *Rag1$^{-/-}$* mice. 5 wk after transplantation, mice were injected with 1 mg tamoxifen for five consecutive days. 5-FU treatment (150 mg/kg) was performed weekly, starting 8 wk after tamoxifen treatment.

KL cells were infected with supernatant from PlatE cells previously transfected with retroviral vectors modulating *Socs3* expression (MSCV-Socs3-Thy1; LMP-shRNA^{Scramble}-GFP, LMP-ShRNA$^{Socs3\#1}$-GFP, and LMP-ShRNA$^{Socs3\#2}$-GFP; Cui

pressing hairpins *Scramble*, *Socs3#1*, and *Socs3#2* were plated in 1 µM methylcellulose$^+$ 4-OH-tamoxifen, and colony-forming activity was determined 9 d after plating (Student's *t* test; *n* = 3). (right) Socs3 expression in colonies generated by CT cells, as determined by immunoblotting. The numbers below the blot indicate the silencing efficiency, as determined by quantifying bands intensity using software analysis. (E) Frequency of the different types of colonies formed by CT and TKO cells transduced with viruses expressing the hairpins *Scramble*, *Socs3#1*, and *Socs3#2* (Student's *t* test; *n* = 3). (F) 4,000 GFP$^+$ TKO cells infected with LMP-GFP retroviral vectors expressing hairpins *Scramble*, *Socs3#1*, and *Socs3#2* were transplanted into conditioned recipient mice together with BM helper cells. Recipient mice were treated with tamoxifen 5 wk after transplantation, and the frequency of GFP$^+$ progenitors (left) and HSC (right) was determined by flow cytometry 9 wk after transplantation (Student's *t* test; *n* = 2 independent experiments with three to five mice per group per experiment). (G) Relative frequency of GFP$^+$ TKO cells transduced with lentiviral vectors expressing hairpins *Scramble* and *Socs3#2* in the BM of recipient mice 30 wk after tamoxifen treatment (Student's *t* test; *n* = 5 mice per group). (H) Conceptual model. In quiescent HSCs, Rb proteins repress the transcriptional activity of E2f factors. Upon transient exit from quiescence, the repressive function of Rb proteins is briefly interrupted, and E2f transcriptional response is restricted to the activation of a cell cycle program. Upon sustained exit from quiescence, E2f transcriptional response expands to genes with non–cell cycle functions such as *Socs3*. Accumulation of Socs3 inhibits Jak2 activity and impairs the homeostasis of proliferative HSCs. Error bars represent standard deviation. *, $P < 0.05$; **, $P < 0.01$; ***, $P < 0.001$.

et al., 2011). 2 d after the final round of infection (two to three rounds were performed, 1 round/d), infected cells (as identified by the expression of Thy1.1 and GFP) were isolated by flow cytometry and transplanted into recipient mice together with 500,000 helper BM cells.

Colony assay

100 CT/TKO HSCs and progenitors and 10,000 unfractioned CT/TKO BM cells were plated in duplicate in 1 ml methylcellulose (STEMCELL Technologies) and 1 μM 4-hydroxy tamoxifen (Fig. S2 B). Colonies were counted after 9–12 d in culture. For serial replating, 10,000 cells were isolated from every condition and replated in duplicates every 9 d. Three independent experiments were performed for each assay and the result from one representative experiment is displayed. For colony assay displayed in Fig. 4 (B and E), flow-isolated KLS cells from untreated CT/TKO mice were infected with retroviruses modulating *Socs3* expression (as described in the previous paragraph), and 250 $Thy1^+$ (Fig. 4 B) and GFP^+ (Fig. 4 E) cells were plated in triplicate in 1 ml methylcellulose and 1 μM 4-hydroxy tamoxifen. Colonies were counted after 9 d in culture. Three independent experiments were performed for each assay, and the mean result from the three experiments is displayed.

Histology and cytospin analysis

Spleen and bone sections were fixed in formalin and mounted, and slides were stained with hematoxylin/eosin. Cytospins were obtained by spinning 20,000 cells at 500 rpm (~30 *g*) against glass slides. Cells were stained with Giemsa, as described previously (Viatour et al., 2008). All histological and morphological analyses were performed by G. Wertheim.

Ex vivo cytokine stimulation

KLS cells, progenitors, and HSCs were flow-isolated from CT and TKO mice 2 wk after tamoxifen treatment and serum-starved for 1 h before stimulation with various amounts of Tpo for 10 min and Sdf1 for 2 min (both PeproTech). Cells were fixed, permeabilized, and stained for either p-Jak2 (Tyr1007-8)/total Jak2 and p-Fak (Tyr397)/total Fak for immunoblotting or anti–p-Stat5 (Tyr694) and p-S6 (Ser235/236; all Cell Signaling Technology) for phospho-flow. KLS cells were flow-isolated and placed in the upper compartment of a Boyden chamber. Cells were allowed to migrate in an Sdf1 gradient for 4 h. After incubation, the cells present in the lower compartment were counted by flow analysis. The data displayed in Fig. 3 (C–E) represent the mean of three independent experiments.

Electrophoretic mobility shift assay, RT-qPCR, ChIP, luciferase assay, and immunoblotting

Molecular biology assays were performed as recently described (Tarangelo et al., 2015). Purified hematopoietic populations were sorted in TRIzol LS, and mRNA was extracted with the direct/zol RNA miniprep kit (Zymo Research), followed by DNaseI digestion to minimize the risk of genomic contamination. Reverse transcription was performed with the ProtoScript First Strand cDNA Synthesis kit (New England Biolabs, Inc.), and qPCR was performed in duplicate with SYBR Green PCR Master Mix (Thermo Fisher Scientific) on the Viia7 Real-Time qPCR system (Thermo Fisher Scientific). Data were normalized using *gapdh* as a reference gene. Primer sequences are available upon request. Each HSC/progenitor sample is a pool of cells collected from three mice to increase cell number.

Electrophoretic mobility shift assay was performed with increasing amount of recombinant GST-E2f1 produced in bacteria and isolated with glutathione beads. Probes were labeled with biotin and detected with streptavidin-conjugated antibody. Competition with a cold E2f consensus probe was performed by incubating increasing amounts of the cold probe before adding the biotin-labeled probe. Annealed probes were run on an agarose gel to confirm similar annealing efficiency.

The vector containing a 1.6-kb fragment of the *Socs3* promoter upstream of the luciferase cDNA was described previously. Four independent luciferase assays were performed, each in duplicate (Jiang et al., 2013). For immunoblotting, unconjugated lysis samples were run on a 4–12% polyacrylamide gel for 1.5 hours at 150 V. Proteins were transferred to a nitrocellulose membrane, blocked in 5% milk for 1 h, and incubated at 4°C with primary antibody overnight. Membrane was washed in TBST three times and probed with an HRP-conjugated secondary antibody (anti–mouse, anti–rabbit, anti–goat) for 1 h. Membrane was washed again three times in TBST. Amplified signal was detected via enhanced chemiluminescence autoradiography. Antibody against Socs3 was purchased from Cell Signaling Technology. For ChIP, ACK-treated primary BM cells and 32D cells were collected into 0.5% SDS lysis buffer at a density of 50×10^6 cells/ml and cross-linked in 2% formaldehyde for 10 min. Lysates were sonicated on a BioLogics Model 3000 Ultrasonic Homogenizer for 30 s at 40% power on ice to produce chromatin fragments of ~400–700 bp. Antibodies against IgG (negative control), E2f1, and E2f3 were purchased from Santa Cruz Biotechnology, Inc.

In silico analysis and statistics

To perform array analysis, cells were isolated in TRIzol and extracted using the QIAGEN RNA miniprep kit. cDNA was amplified before array analysis (Stanford Functional Genomics Facility, Stanford, CA). Array data generated in this publication are publicly available (GEO accession no. GSE98311). In short, GMAP/GSNAP was used to align the fragments to mouse assembly GRCm38. Normalization and differential expression analysis was performed with the Bioconductor package "DESeq2." Microarray data were obtained from GEO with accession nos. GSE1559 (Figs. 2 K and 3 I) and GSE11253 (Fig. 3, G and H). All microarray data were processed and normalized with the RMA algorithm implemented in the "affy" R package. Heat maps for both microarrays and RNA-Seq were plotted using R packages "pheatmap" and "ggplot2."

Online supplemental material

Fig. S1 shows CT HSCs and progenitor cells are immunophenotypically and functionally undistinguishable from WT counterparts. Fig. S2 shows impaired homeostasis of TKO HSCs. Tables S1–S7 are included in a separate Excel file. Table S1 shows gene profiling in TKO versus CT HSCs. Table S2 shows GSEA for genes up-regulated in TKO versus CT HSCs. Table S3 shows GSEA for genes down-regulated in TKO versus CT HSCs. Table S4 shows genes up-regulated only in TKO versus CT HSCs. Table S5 shows genes up-regulated only in TKO versus CT KLS cells. Table S6 shows genes up-regulated in both TKO HSCs and KLS cells versus their respective controls. Table S7 shows the cell cycle signature in TKO HSCs and KLS cells versus their respective controls.

ACKNOWLEDGMENTS

We thank the members of the Cancer PathoBiology Division of the Department of Pathology at CHOP, as well as Peter Klein, Warren Pear, and Ken Zaret for their suggestions and their critical reading of the manuscript. We thank Nathanael Lo and Rebecca Teng for excellent technical work. We thank Susan Kaech and Frank Gonzalez for the kind gift of vectors to modulate *Socs3* expression and the luciferase vector containing *Socs3* promoter, respectively. We also thank the members of the Flow Cytometry and Animal Facility at CHOP.

P. Viatour is supported by the W.W. Smith Charitable Trust, a Foerderer Award, the Alex's Lemonade Stand Foundation, the Canuso Foundation, the American Cancer Society (grant RSG-16-233-01-TBE), and start-up funds from the Center for Childhood Cancer Research at the Children's Hospital of Philadelphia.

The authors declare no competing financial interests.

Submitted: 18 May 2016

Revised: 30 January 2017

Accepted: 1 May 2017

REFERENCES

Akada, H., S. Akada, R.E. Hutchison, K. Sakamoto, K.U. Wagner, and G. Mohi. 2014. Critical role of Jak2 in the maintenance and function of adult hematopoietic stem cells. *Stem Cells.* 32:1878–1889. http://dx.doi.org/10.1002/stem.1711

Anthony, B.A., and D.C. Link. 2014. Regulation of hematopoietic stem cells by bone marrow stromal cells. *Trends Immunol.* 35:32–37. http://dx.doi.org/10.1016/j.it.2013.10.002

Bersenev, A., C. Wu, J. Balcerek, and W. Tong. 2008. Lnk controls mouse hematopoietic stem cell self-renewal and quiescence through direct interactions with JAK2. *J. Clin. Invest.* 118:2832–2844. http://dx.doi.org/10.1172/JCI35808

Burkhart, D.L., and J. Sage. 2008. Cellular mechanisms of tumour suppression by the retinoblastoma gene. *Nat. Rev. Cancer.* 8:671–682. http://dx.doi.org/10.1038/nrc2399

Busch, K., K. Klapproth, M. Barile, M. Flossdorf, T. Holland-Letz, S.M. Schlenner, M. Reth, T. Höfer, and H.R. Rodewald. 2015. Fundamental properties of unperturbed haematopoiesis from stem cells in vivo. *Nature.* 518:542–546. http://dx.doi.org/10.1038/nature14242

Cao, A.R., R. Rabinovich, M. Xu, X. Xu, V.X. Jin, and P.J. Farnham. 2011. Genome-wide analysis of transcription factor E2F1 mutant proteins reveals that N- and C-terminal protein interaction domains do not participate in targeting E2F1 to the human genome. *J. Biol. Chem.* 286:11985–11996. http://dx.doi.org/10.1074/jbc.M110.217158

Capello, D., C. Deambrogi, D. Rossi, T. Lischetti, D. Piranda, M. Cerri, V. Spina, S. Rasi, G. Gaidano, and M. Lunghi. 2008. Epigenetic inactivation of suppressors of cytokine signalling in Philadelphia-negative chronic myeloproliferative disorders. *Br. J. Haematol.* 141:504–511. http://dx.doi.org/10.1111/j.1365-2141.2008.07072.x

Casola, S. 2010. Mouse models for miRNA expression: The ROSA26 locus. *Methods Mol. Biol.* 667:145–163. http://dx.doi.org/10.1007/978-1-60761-811-9_10

Chen, H.Z., S.Y. Tsai, and G. Leone. 2009. Emerging roles of E2Fs in cancer: An exit from cell cycle control. *Nat. Rev. Cancer.* 9:785–797. http://dx.doi.org/10.1038/nrc2696

Cui, W., Y. Liu, J.S. Weinstein, J. Craft, and S.M. Kaech. 2011. An interleukin-21-interleukin-10-STAT3 pathway is critical for functional maturation of memory CD8+ T cells. *Immunity.* 35:792–805. http://dx.doi.org/10.1016/j.immuni.2011.09.017

de Graaf, C.A., and D. Metcalf. 2011. Thrombopoietin and hematopoietic stem cells. *Cell Cycle.* 10:1582–1589. http://dx.doi.org/10.4161/cc.10.15619

Glodek, A.M., Y. Le, D.M. Dykxhoorn, S.Y. Park, G. Mostoslavsky, R. Mulligan, J. Lieberman, H.E. Beggs, M. Honczarenko, and L.E. Silberstein. 2007. Focal adhesion kinase is required for CXCL12-induced chemotactic and pro-adhesive responses in hematopoietic precursor cells. *Leukemia.* 21:1723–1732. http://dx.doi.org/10.1038/sj.leu.2404769

Jiang, C., J.H. Kim, F. Li, A. Qu, O. Gavrilova, Y.M. Shah, and F.J. Gonzalez. 2013. Hypoxia-inducible factor 1α regulates a SOCS3-STAT3-adiponectin signal transduction pathway in adipocytes. *J. Biol. Chem.* 288:3844–3857. http://dx.doi.org/10.1074/jbc.M112.426338

Kershaw, N.J., J.M. Murphy, N.P. Liau, L.N. Varghese, A. Laktyushin, E.L. Whitlock, I.S. Lucet, N.A. Nicola, and J.J. Babon. 2013. SOCS3 binds specific receptor-JAK complexes to control cytokine signaling by direct kinase inhibition. *Nat. Struct. Mol. Biol.* 20:469–476. http://dx.doi.org/10.1038/nsmb.2519

Kimura, S., A.W. Roberts, D. Metcalf, and W.S. Alexander. 1998. Hematopoietic stem cell deficiencies in mice lacking c-Mpl, the receptor for thrombopoietin. *Proc. Natl. Acad. Sci. USA.* 95:1195–1200. http://dx.doi.org/10.1073/pnas.95.3.1195

Le, Y., B.M. Zhu, B. Harley, S.Y. Park, T. Kobayashi, J.P. Manis, H.R. Luo, A. Yoshimura, L. Hennighausen, and L.E. Silberstein. 2007. SOCS3 protein developmentally regulates the chemokine receptor CXCR4-FAK signaling pathway during B lymphopoiesis. *Immunity.* 27:811–823. http://dx.doi.org/10.1016/j.immuni.2007.09.011

Li, Y., J. McClintick, L. Zhong, H.J. Edenberg, M.C. Yoder, and R.J. Chan. 2005. Murine embryonic stem cell differentiation is promoted by SOCS-3 and inhibited by the zinc finger transcription factor Klf4. *Blood.* 105:635–637. http://dx.doi.org/10.1182/blood-2004-07-2681

Marine, J.C., C. McKay, D. Wang, D.J. Topham, E. Parganas, H. Nakajima, H. Pendeville, H. Yasukawa, A. Sasaki, A. Yoshimura, and J.N. Ihle. 1999. SOCS3 is essential in the regulation of fetal liver erythropoiesis. *Cell.* 98:617–627. http://dx.doi.org/10.1016/S0092-8674(00)80049-5

Meyer, S.C., and R.L. Levine. 2014. Molecular pathways: Molecular basis for sensitivity and resistance to JAK kinase inhibitors. *Clin. Cancer Res.* 20:2051–2059. http://dx.doi.org/10.1158/1078-0432.CCR-13-0279

Morrison, S.J., and D.T. Scadden. 2014. The bone marrow niche for haematopoietic stem cells. *Nature.* 505:327–334. http://dx.doi.org/10.1038/nature12984

O'Malley, D.P., Y.S. Kim, S.L. Perkins, L. Baldridge, B.E. Juliar, and A. Orazi. 2005. Morphologic and immunohistochemical evaluation of splenic hematopoietic proliferations in neoplastic and benign disorders. *Modern Pathology.* 18:1550–1561.

Orford, K.W., and D.T. Scadden. 2008. Deconstructing stem cell self-renewal: Genetic insights into cell-cycle regulation. *Nat. Rev. Genet.* 9:115–128. http://dx.doi.org/10.1038/nrg2269

Passegué, E., A.J. Wagers, S. Giuriato, W.C. Anderson, and I.L. Weissman. 2005. Global analysis of proliferation and cell cycle gene expression in the regulation of hematopoietic stem and progenitor cell fates. *J. Exp. Med.* 202:1599–1611. http://dx.doi.org/10.1084/jem.20050967

Pello, O.M., M.C. Moreno-Ortiz, J.M. Rodríguez-Frade, L. Martínez-Muñoz, D. Lucas, L. Gómez, P. Lucas, E. Samper, M. Aracil, C. Martínez, et al. 2006. SOCS up-regulation mobilizes autologous stem cells through CXCR4 blockade. *Blood.* 108:3928–3937. http://dx.doi.org/10.1182/blood-2006-02-006353

Pietras, E.M., M.R. Warr, and E. Passegué. 2011. Cell cycle regulation in hematopoietic stem cells. *J. Cell Biol.* 195:709–720. http://dx.doi.org/10.1083/jcb.201102131

Staerk, J., and S.N. Constantinescu. 2012. The JAK-STAT pathway and hematopoietic stem cells from the JAK2V617F perspective. *JAK-STAT.* 1:184–190. http://dx.doi.org/10.4161/jkst.22071

Sugiyama, T., H. Kohara, M. Noda, and T. Nagasawa. 2006. Maintenance of the hematopoietic stem cell pool by CXCL12-CXCR4 chemokine signaling in bone marrow stromal cell niches. *Immunity.* 25:977–988. http://dx.doi.org/10.1016/j.immuni.2006.10.016

Sun, J., A. Ramos, B. Chapman, J.B. Johnnidis, L. Le, Y.J. Ho, A. Klein, O. Hofmann, and F.D. Camargo. 2014. Clonal dynamics of native haematopoiesis. *Nature.* 514:322–327. http://dx.doi.org/10.1038/nature13824

Tarangelo, A., N. Lo, R. Teng, E. Kim, L. Le, D. Watson, E.E. Furth, P. Raman, U. Ehmer, and P. Viatour. 2015. Recruitment of Pontin/Reptin by E2f1 amplifies E2f transcriptional response during cancer progression. *Nat. Commun.* 6:10028. http://dx.doi.org/10.1038/ncomms10028

Tong, W., Y.M. Ibarra, and H.F. Lodish. 2007. Signals emanating from the membrane proximal region of the thrombopoietin receptor (mpl) support hematopoietic stem cell self-renewal. *Exp. Hematol.* 35:1447–1455. http://dx.doi.org/10.1016/j.exphem.2007.05.010

Venezia, T.A., A.A. Merchant, C.A. Ramos, N.L. Whitehouse, A.S. Young, C.A. Shaw, and M.A. Goodell. 2004. Molecular signatures of proliferation and quiescence in hematopoietic stem cells. *PLoS Biol.* 2:e301. http://dx.doi.org/10.1371/journal.pbio.0020301

Viatour, P., T.C. Somervaille, S. Venkatasubrahmanyam, S. Kogan, M.E. McLaughlin, I.L. Weissman, A.J. Butte, E. Passegué, and J. Sage. 2008. Hematopoietic stem cell quiescence is maintained by compound contributions of the retinoblastoma gene family. *Cell Stem Cell.* 3:416–428. http://dx.doi.org/10.1016/j.stem.2008.07.009

Vila-Coro, A.J., J.M. Rodríguez-Frade, A. Martín De Ana, M.C. Moreno-Ortíz, C. Martínez-A, and M. Mellado. 1999. The chemokine SDF-1alpha triggers CXCR4 receptor dimerization and activates the JAK/STAT pathway. *FASEB J.* 13:1699–1710.

Wang, Z., G. Li, W. Tse, and K.D. Bunting. 2009. Conditional deletion of STAT5 in adult mouse hematopoietic stem cells causes loss of quiescence and permits efficient nonablative stem cell replacement. *Blood.* 113:4856–4865. http://dx.doi.org/10.1182/blood-2008-09-181107